SPECIAL
CAHMDA III
COLLECTION

Ability to Forecast Regional Soil Moisture with a Distributed Hydrological Model Using ECMWF Rainfall Forecasts

J. M. Schuurmans* and M. F. P. Bierkens

Department of Physical Geography, Utrecht University, Utrecht, The Netherlands

ABSTRACT

This study mimics an online forecast system to provide nine day-ahead forecasts of regional soil moisture. It uses modified ensemble rainfall forecasts from the numerical weather prediction model of the European Centre for Medium-Range Weather Forecasts (ECMWF), which is provided by the Royal Netherlands Meteorological Office (KNMI). Both the individual ensembles as well as the mean of the ensembles are used as input for a hydrological model of a 70-km^2 study area during March–November 2006. The outcomes are compared to the model run with high-resolution rainfall fields (based on 14 rain gauges within the study area and meteorological radar) as input. It is shown that the total spatial mean rainfall is forecasted very well for all lead times. The measured rainfall (spatial mean) shows a distribution with peaks at 0–1 and >10 mm day^{-1}. These peaks are underestimated by the ensemble mean of the forecasts and this underestimation increases with lead time. This is not the case when ensemble members are used. Besides, the modeled uncertainty in rainfall by ECMWF underestimates the true uncertainty for all lead times and the number of rainfall events (thresholds 0.1, 0.5, and 1.0 mm) is overestimated. Absolute temporal mean bias values in root zone storage—that is, soil moisture—larger than 1 mm start to show for lead times longer than 3 days. The lower and upper bounds of bias for a lead time of 9 days are approximately −4 and 7 mm, respectively (negative values mean the forecasted soil moisture is underestimated). The bias in root zone storage shows a spatial pattern that represents the spatial pattern of total rainfall: areas with less rainfall than spatial average show a negative bias and vice versa. Local differences within this spatial pattern are due to land use and soil type. The results suggest that ensemble forecasts of soil moisture using ensemble rainfall forecasts from ECMWF are of practical use for water management, even at regional scales.

1. Introduction

Insight into the spatial distribution of soil moisture within a catchment is of great importance to many groups, for example, farmers and water management boards. Accurate short- to medium-range prediction of spatially distributed soil moisture is helpful for optimizing irrigation gifts, forecasting hydrological drought, and assessing catchment wetness for flood control. Because rainfall is one of the most important input variables in hydrological models, the accuracy of the soil moisture prediction depends highly on the accuracy of the rainfall forecast.

Recent studies successfully used ensemble rainfall predictions from numerical weather prediction (NWP) models in hydrological models (e.g., Roo et al. 2003; Gouweleeuw et al. 2005; Olsson and Lindström 2008; Pappenberger et al. 2005; Roulin and Vannitsem 2005; Roulin 2007). However, these studies all focus on the prediction of discharge.

In this study we use rainfall forecasts from the Ensemble Prediction System (EPS) of the European Centre for Medium-Range Weather Forecasts (ECMWF) as input for a spatially distributed hydrological model focusing on soil moisture instead of discharge. The ECMWF EPS system produces six hourly rainfall outputs in the form of an operational run, a control run, and 50 ensembles. The operational run is the full model run at high resolution. The control run has the same input conditions as the operational run; however, for calculation time reduction the model resolution is lower. The 50 ensembles are produced by perturbing

_____

* Current affiliation: FutureWater, Wageningen, Netherlands.

_____

Corresponding author address: J. M. Schuurmans, FutureWater, Costerweg 1G, Wageningen 6702 AA, Netherlands.
E-mail: h.schuurmans@futurewater.nl

the initial state of the control run. All ensemble members are equally likely to occur (Persson 2001). The scope of this study is to verify the ability to forecast the spatial distribution of soil moisture using EPS rainfall forecasts.

Our hydrological model simulates the water flow in both the unsaturated and saturated zone of a 70-km^2 catchment in the Netherlands. Within this catchment rainfall is measured using meteorological radar and 14 rain gauges within the catchment. ECMWF forecasts, provided by the Royal Netherlands Meteorological Office (KNMI), are compared with measured rainfall from radar and rain gauges. Ensemble hydrological model runs are performed using each ensemble member of the rainfall forecast as input. Also, the ensemble mean is used as input for our hydrological model. The output from each forecasting system is compared with output from the hydrological model forced with the observed rainfall data.

The remainder of this paper is organized as follows. Section 2 starts with a description of the ensemble soil moisture prediction system. The study area is described in section 2b. Details about the hydrological model are given in section 2c. Section 2d describes the rainfall data used, both measured rainfall as well as the rainfall forecasts. Section 3 gives the results, both for the rainfall accuracy (section 3a) and for the soil moisture accuracy (section 3b). Section 4 lists the main conclusions of this study and points out the opportunities for further research.

2. Method and data

a. Ensemble soil moisture prediction system

Six hourly ECMWF EPS rainfall forecasts during the period March–November 2006 are provided by the KNMI. We accumulated these forecasts to daily forecasts with a time span of 0600–0600 UTC, resulting in nine daily rainfall forecasts [lead times (lt) 1–9 days]. These daily forecasts (both the individual ensemble members and the ensemble mean) are compared with measured rainfall that has a time span of 0800–0800 UTC (rainfall fields estimated with both radar and rain gauges). The error caused by the 2-h difference in time span is investigated in section 2d.

We use two different soil moisture forecast systems.

(I) Each ensemble member of the rainfall forecast is used as input for the hydrological model. This gives each day 50 realizations of soil moisture for lead time from 1 day (lt1) up to 9 days (lt9);

(II) The ensemble mean of the rainfall forecast is used as input for the hydrological model. This gives

each day one realization of soil moisture for lead time from lt1 up to lt9.

The reason why we use these two different soil moisture forecast systems is because the unsaturated zone of our hydrological model is a nonlinear system. The computational costs of system II are significantly lower than those of system I. Therefore, it is interesting to investigate the difference between the mean of the soil moisture ensemble members calculated with system I and the soil moisture calculated with system II. However, if we want to show the reliability—that is, consistency—of predicted soil moisture or want to make probabilistic forecasts, we need to run system I.

The model is also run with measured (spatially variable) rainfall as input, hereafter "true run." Results of forecasted soil moisture are compared to the true run per lead time. For each forecast run, the initial values from the true run were set for the unsaturated and saturated zones. The input for reference evapotranspiration was set at their observed values. In reality this should also be set at the forecasted values. However, we are interested in the effect of rainfall forecast and these results should be considered as the upper bound of skill of the system.

b. Study area

Our study area is called the Langbroekerwetering, which lies in the central part of the Netherlands (Fig. 1a). The Langbroekerwetering (~70 km^2) is located along the rim of the Holocene Rhine–Meuse delta (low elevation and peat and clay of the last 4000 yr; Berendsen and Stouthamer 2000), which onlaps coversands and sandur outwash deposits in front of a Saalian ice-pushed ridge (high elevation and 150 000 yr old; Busschers et al. 2007). Figure 1b shows the elevation together with the location of the rain gauges and the soil moisture measurements, land use, and soil types of the Langbroekerwetering. For a description of the soil types, we refer to Table 1. At the higher elevations coarse sand forest dominates the area, whereas in the lower area grassland dominates. Some small villages (built-up area) are located within the area. The land use map is derived from the Dutch national land cover database LGN (van Oort et al. 2004; de Wit and Clevers 2004).

c. Hydrological model

The model used in this study is a coupled groundwater (saturated zone) and unsaturated zone model, hereafter metaswap. The groundwater model is based on the Modular Three-Dimensional Groundwater Flow Model (MODFLOW) model code (McDonald and Harbaugh 1984). The unsaturated zone model is a
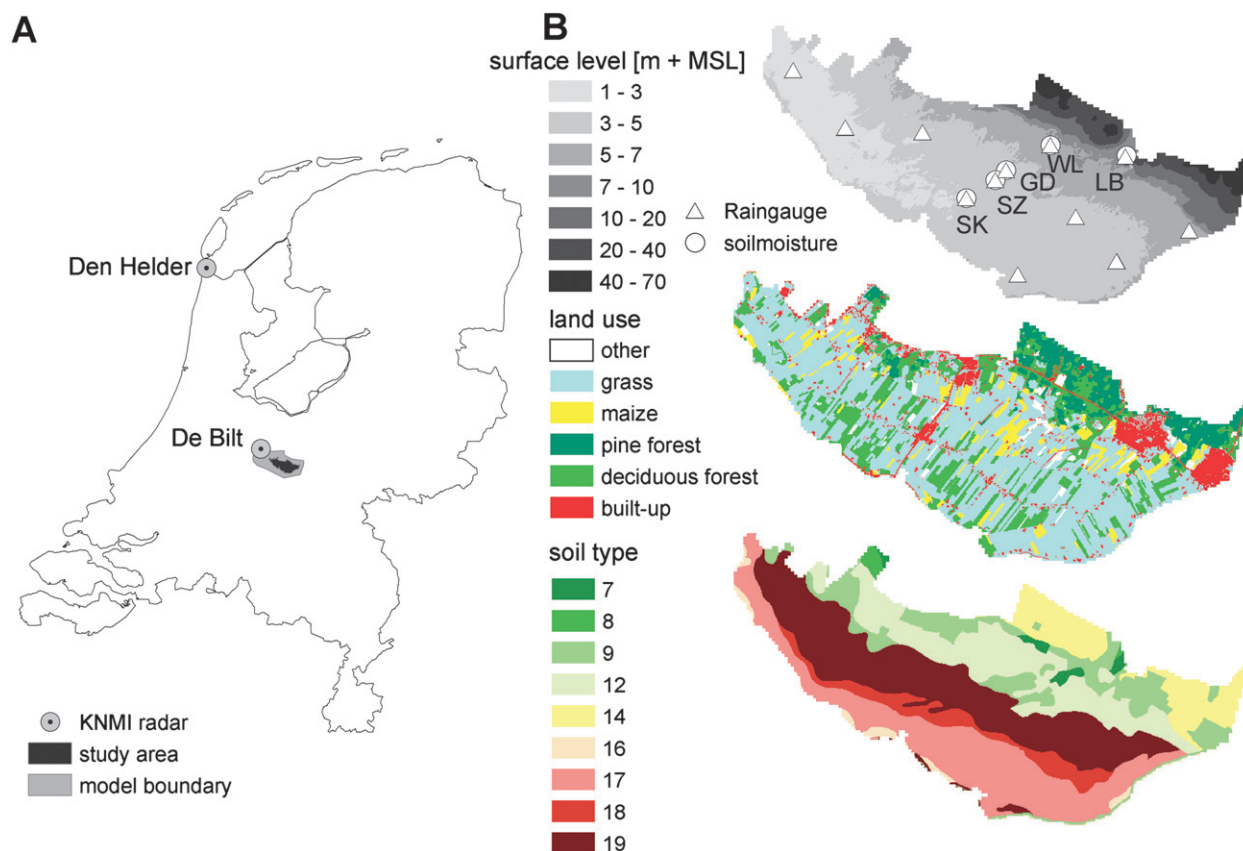
FIG. 1. (a) Location of study area as well as model boundary within the Netherlands, and the location of the two rainfall radars. (b) Surface level (m + mean sea level) with rain gauge and soil moisture locations, land use, and soil types (see Table 1) of the study area.

quasi-steady-state model that uses a sequence of steady-state water content profiles for dynamic simulation (van Walsum and Groenendijk 2008). The steady-state water content profiles were obtained by running a steady-state version of the swap model (van Dam 2000) offline. The model area is divided into soil–vegetation–atmosphere transfer (SVAT) units, which are smaller or equal to the size of the MODFLOW cell. One MODFLOW cell can be coupled to several SVAT units. The SVAT units form parallel vertical columns, which are divided into a root zone (part of the unsaturated zone where extraction of water by roots occurs) and a subsoil layer (part of the unsaturated zone where interchange with saturated zone takes place). Metaswap distinguishes between 21 different soil types. For each soil type, the model has predefined sublayers with corresponding soil physical parameters (also called Van Genuchten parameters) to be able to convert pressure head to soil moisture content. Only vertical flow according to Richard's equation is taken into account. All lateral exchanges are assumed to take place in the saturated zone. The thickness of the root zone is user specified. In this study we use a

thickness of 0.3 for grassland and built up area, 0.6 for maize, and 1.0 m for forest.

In our model, the size of the MODFLOW cells is 100×100 m. The SVAT units have a resolution of 25×25 inside the study area and 100×100 m outside the study area, within the model boundaries (Fig. 1a). The groundwater model is schematized into seven layers.

A flux that is of importance for soil moisture and is influenced by the soil moisture conditions is

TABLE 1. Description of soil types within study area (Wösten et al. 1995).

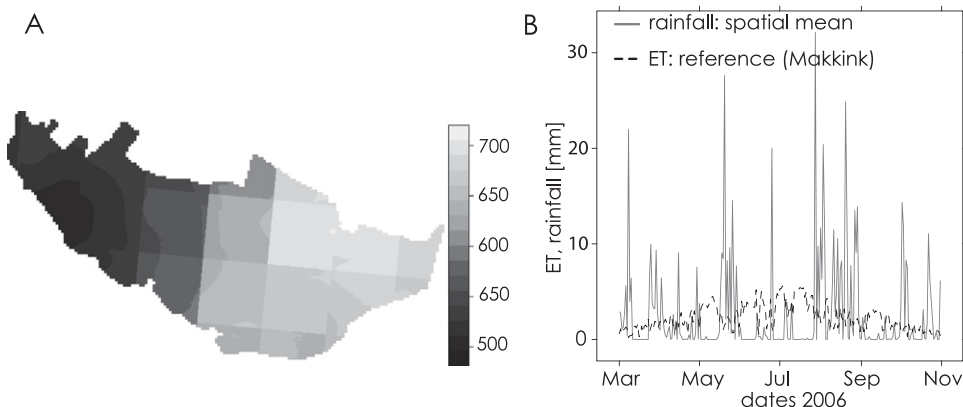| Soil unit	Description
7	Drift sand
8	Podzol in loam poor fine sand
9	Podzol in loamy fine sand
12	Enkeerd in loamy fine sand
14	Podzol in coarse sand
16	Light clay
17	Clay with heavy layers
18	Clay on peat
19	Clay on sand

A

B

FIG. 2. (a) Spatial distribution of accumulated rainfall (mm) March–November 2006 and (b) time series of the spatial mean of rainfall within the study area and the reference evapotranspiration.

evapotranspiration. Our model uses Makkink (Bruin 1987; Makkink 1957; Winter et al. 1995) reference evapotranspiration (ET_{ref}) as input (spatially uniform). The measured ET_{ref} in this study comes from De Bilt. The potential evapotranspiration (ET_{pot}) is calculated by multiplying ET_{ref} with a crop factor that is related to the land use type and can vary throughout the season (in our model, 1.0 throughout the season for grassland and forest; 0–1.3 for maize, and 0.05 for the built-up area). The actual evapotranspiration (ET_{act}) is equal or a fraction of ET_{pot}, depending on soil moisture conditions and land use type. Also, interception evaporation occurs in forest areas. The interception capacity for pine forest is set to 1.0 throughout the season and 0.3–1.0 mm m^{-2} for deciduous forest depending on the season.

d. Rainfall data

The measured rainfall is a combination of meteorological radar and rain gauges within and closely around the model area. The interpolation method used is a geostatistical method that combines radar estimates with rain gauge observations. The method makes use of collocated cokriging and is explained in more detail in Schuurmans et al. (2007). Figure 2a shows the spatial distribution of the rainfall accumulated during March–November 2006 within the study area. There is up to 200-mm difference during this eight-month period within 15 km, which is even more than that found in 2004 in another equally sized catchment (50–100 mm during a seven-month period; Schuurmans and Bierkens 2007). Figure 2b shows the time series of the spatial mean rainfall within the study area and the reference evapotranspiration.

The ECMWF EPS rainfall forecasts within the Netherlands were interpolated by the KNMI to a regular 0.5° × 0.5° grid. For this study we used the forecasts

at 0000 UTC with a time step of 6 h nearest to De Bilt (Fig. 1a) and accumulated these to daily rainfall. As mentioned in section 2a, the time span of the forecasts is 0600–0600 UTC, whereas the time span of the measured rainfall is 0800–0800 UTC. We investigated the error caused by the difference in time span using the automatic rain gauge at De Bilt that recorded hourly data. Figure 3 shows per day the amount of rainfall that should be added to the time span of the 0600–0600 UTC to get the same amount during 0800–0800 UTC (solid line). The measured rainfall (0800–0800 UTC) is also shown (dashed line). In 10% of the days the difference was not zero, and the maximum was 6.5 mm. This difference was ignored in this study.
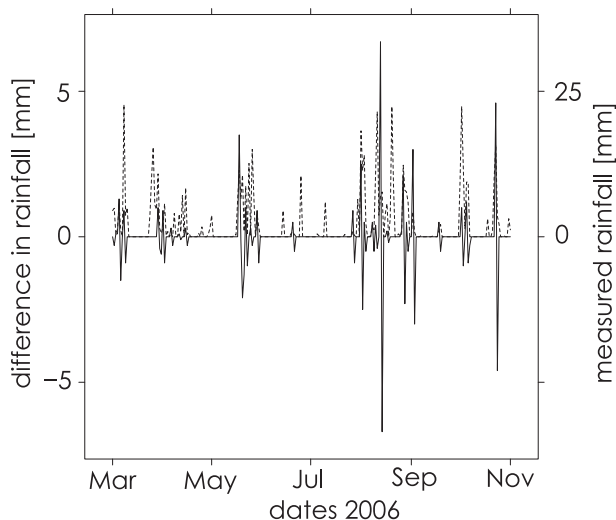

FIG. 3. Difference in rainfall depth (mm) due to the difference in time span between the forecasts and the measured rainfall (solid line) as well as the measured daily (0800–0800 UTC) rainfall (dashed line). Hourly data comes from the De Bilt rain gauge station.
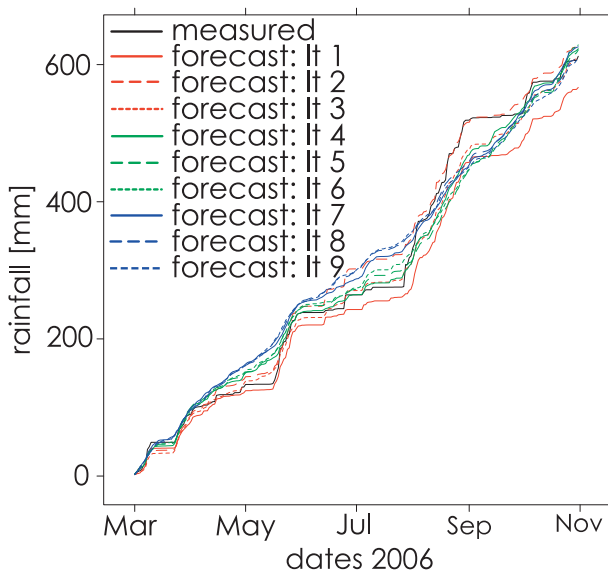
FIG. 4. Cumulative rainfall distribution of the measured (spatial mean) and the forecasted (ensemble mean) rainfall for lt1–lt9.

3. Results and discussion

a. ECMWF rainfall accuracy

Figure 4 shows the cumulative rainfall distribution of the measured (spatial mean) and forecasted (ensemble mean) rainfall per lead time. Table 2 shows the total rainfall amount during the study period of measured and forecasted rainfall. The total amount of rainfall during the study period is forecasted within 3% of the measured rainfall except for lt1, which is 7% less than measured rainfall.

The distribution of measured and forecasted daily rainfall over different ranges is shown in Fig. 5. Figure 5a is based on the ensemble mean, Fig. 5b is based on the ensemble members. For most of the days (~60%), the spatial mean measured rainfall within the study area was between 0 and 1, followed by >10 mm day^{-1} (~10%). Figure 5a shows that for the forecasted rainfall based on ensemble mean, the percentage of days with 0–1 mm day^{-1} gradually decreases with increasing lead time. This phenomena also occurs for events with >10 mm day^{-1}. However, when using the ensemble members, the forecasted rainfall follows more or less the distribution of measured rainfall for all lead times. This suggests that it is better to use the ensemble members because the ensemble mean is apparently used to smooth a representation of rainfall variability. This smoothing effect increases with lead time, which is due to the larger spread between ensemble members, making the ensemble mean closer to climatological mean.

TABLE 2. Total rainfall during March–November 2006 according to measurements (spatial mean) and forecasts (ensemble mean) for lead time (lt) 1–9 days.

Measured	lt1	lt2	lt3	lt4	lt5	lt6	lt7	lt8	lt9
612	567	629	612	623	621	629	626	611	609

Figure 6 shows a medley of statistics for forecasted rainfall—that is, bias, root-mean-square error (RMSE), mean absolute error (MAE), and correlation (r^2) between measured (spatial mean) and forecasted rainfall are plotted per lead time. Also, the ensemble spread (temporal mean standard deviation of ensemble members), which is a measure for the rainfall forecast reliability, is shown vs lead time. For completeness, we also included RMSE, MAE, and r^2 calculated from the ensemble members. The RMSE and MAE of the ensemble mean increase and the correlation decreases with lead time. The bias, however, remains more or less constant around zero with lead time, which means that under-and overestimation of rainfall are compensated, which can also be seen in Fig. 4.

As expected the RMSE and MAE of the ensemble members is higher than the RMSE and MAE of the mean, whereas r^2 is lower. In fact, if observations and ensemble members are assumed to be realizations of the same underlying stochastic process and the bias is zero, RMSE of the ensembles members should be in theory $\sqrt{2}$ (~1.4) as large as that of RMSE of the ensemble mean. The ensemble spread increases, and thus the rainfall forecast reliability decreases, with lead time. However, comparing the ensemble spread with the RMSE of the ensemble mean and noticing the bias is close to zero, we must conclude that the modeled uncertainty underestimates the true uncertainty of the forecast for all lead times. A possible explanation is that the ensemble forecasts only consider the uncertainty of initial conditions, whereas model errors (e.g., rainfall parameterization and scale discrepancy between atmosphere model and catchment) yield additional errors.

We used Table 3 to calculate the categorical measures of skill, which indicate how well rainfall events are predicted (Johnson and Olson 1998). Figure 7 shows the bias ratio, probability of detection (POD), critical success index (CSI), and false alarm rate (FAR). Bias ratio is the ratio between predicted and observed rainfall events [$= (F+H)/(M+H)$]. POD [$= H/(M+H)$] gives the fraction of rainfall events that are successfully forecasted. CSI [$= H/(M+H+F)$] is the number of hits divided by hits, misses, and false alarms. FAR [$= F/(F+H)$] indicates how often rainfall events are predicted but not observed. In a forecast without bias, the bias ratio equals 1 (POD + FAR = 1). In a perfect
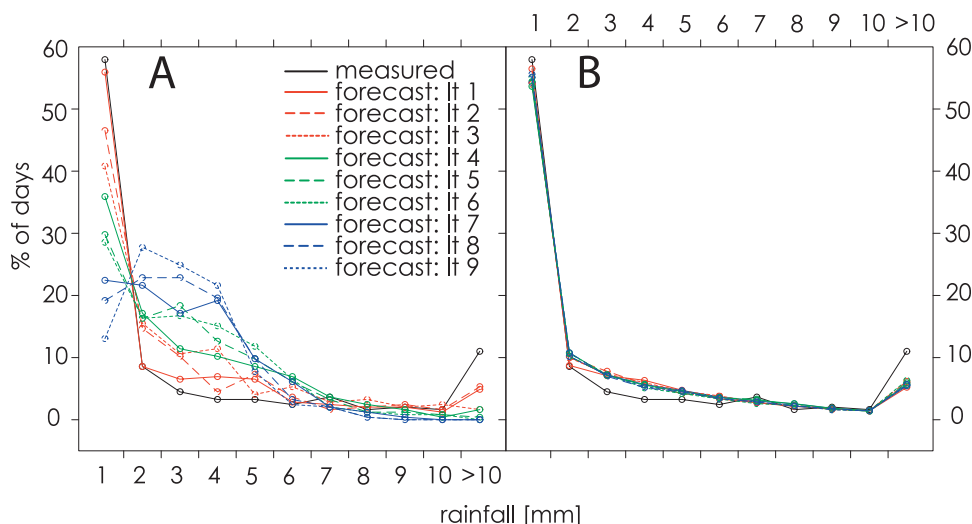
FIG. 5. Percentage of days as a function of rainfall amount for the measured (spatial mean) and forecasted rainfall for lt1–lt9 based on: (a) ensemble mean and (b)ensemble members.

forecast, POD = 1, CSI = 1, and FAR = 0. The measures of skill were calculated for both the ensemble mean as well as for all the individual ensemble members. For the observed rainfall, we use the spatial mean rainfall. Three different thresholds are taken (0.1, 0.5, and 1.0 mm day^{-1}) to indicate a rainfall event. The motivation for the choice of these thresholds is the detection limit of conventional tipping bucket rain gauges (0.1 mm day^{-1}) and the interception capacity of forest in our model (1.0 mm m^{-2} throughout the season for pine forest and 0.3–1.0 mm m^{-2} for deciduous forest). Figure 7a shows a strong increase of bias ratio with lead time for the ensemble mean, especially for the higher threshold. For the individual ensemble members, the bias ratio is more or less constant (~1.3) with lead time for all the thresholds. Also, for POD and FAR we see a difference between the ensemble mean and the individual ensemble members. As could be expected, the ensemble mean leads to an increase in the number of forecasted rain events, which means that bias ratio, POD, and FAR are higher for the ensemble mean than for the individual ensemble members. The POD based on the ensemble mean is more or less constant (~1) with lead time for all the thresholds. However, based on the individual ensemble members, POD decreases with lead time, especially for higher thresholds. CSI decreases with lead time (especially for higher thresholds) but shows hardly any difference between ensemble mean and ensemble members. FAR increases with lead time, especially for higher thresholds. The differentiation of bias ratio, POD, and FAR between ensemble mean and individual ensemble members with increasing lead time can be explained by the increase of en-

semble spread with increasing lead time, as shown in Fig. 6.

b. Soil moisture accuracy

As mentioned in section 2a, we use two different soil moisture forecast systems. We compare per lead time, the difference between the forecasted storage in root zone and the storage in root zone according to the true run. Figure 8 shows the bias (temporal mean during the study period) if the true run is compared to the mean of the forecasted soil moisture ensembles (system I). Positive bias values mean the forecast underestimates the root zone storage of the true run. Figure 9 shows the same, but this time the true run is compared with the
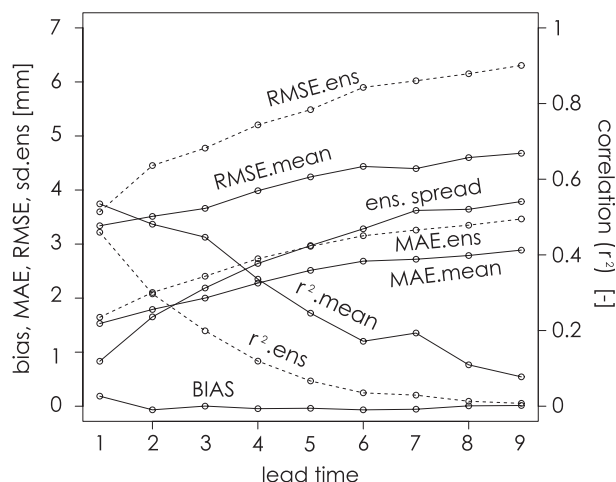

FIG. 6. Rainfall forecast statistics vs lead time.

TABLE 3. Categories of rainfall prediction used to calculate categorical measures of skill. A threshold of 0.1 mm day^{-1} is used to indicate a rainfall event.

	Predicted: no rain	Predicted: rain
Observed: no rain	Z	F
Observed: rain	M	H

storage in root zone from the run with the ensemble mean of the rainfall forecast as input (system II). For both systems the bias increases with lead time. Absolute bias values >1 mm begin to show around lt3. The lower and upper bounds of bias at lt9 are approximately −4 and 7 mm, respectively. For both systems we see a spatial pattern in the bias that becomes more pronounced with increasing lead time. The spatial pattern of the bias in root zone storage strongly resembles the spatial pattern of total rainfall (Fig. 2a). The area with less rainfall than the spatial average (i.e., the western part of the study area) shows a negative bias, whereas the area with more rainfall than the spatial average—that is, the eastern part—shows a positive bias. This can be explained by the true run being forced with spatially variable rainfall, whereas the rainfall forecasts are spatially uniform. In the western part of the study area, more rainfall falls according to the forecasts, which leads to higher values in root zone storage and thus to negative bias (and vice versa for the eastern part). Local differences occur that are superimposed on this overall bias spatial pattern, which can be attributed to differences in land use and soil type. If we compare Figs. 8 and 9 with the pattern of land use in Fig. 1b, we see that forest exhibits locally higher values of bias in root zone storage—that is, the underestimation of forecasted soil moisture. We think that the reason for this underesti-

mation of forecasted soil moisture in areas with forest lies in the overestimation of the interception (evaporation) in these areas. As shown in section 3a, the total rainfall is almost the same for each lead time but the events with high rainfall intensity are underestimated, whereas the number of rain events (thresholds 0.1, 0.5, and 1.0 mm day^{-1}) are overestimated (FAR > 1; Fig. 7). In reality, however, increased occurrence of rain could go together with reduced evapotranspiration (because of more clouds and thus reduced solar radiation). This effect is not taken into account because we use observed evapotranspiration in our soil moisture forecast system. Built-up areas show no bias within a region of positive bias (northeast). This is not surprising because in built-up areas, there is hardly any relationship between rainfall and soil moisture because rainfall does not infiltrate (either because of drainage or low infiltration capacity). We also see some differences in bias in root zone storage in areas with the same land use but with different soil types, which suggests that soil type plays a role as well.

Table 4 gives the spatial mean values of the temporal mean bias, RMSE, and MAE of root zone storage for both forecast systems for each lead time. Figure 10 shows in the box-and-whisker plots the spatial distribution of the temporal mean bias in root zone storage for both soil moisture forecast systems (system I in white and system II in gray) per lead time. From this table and figure, it can be concluded that it doesn't make much difference whether one uses soil moisture forecast system I or II, although system I gives slightly better results than system II. However, with system I it is possible to make probabilistic forecasts and to show per SVAT unit the uncertainty of the predicted storage in root zone. As an example, we show for one SVAT unit
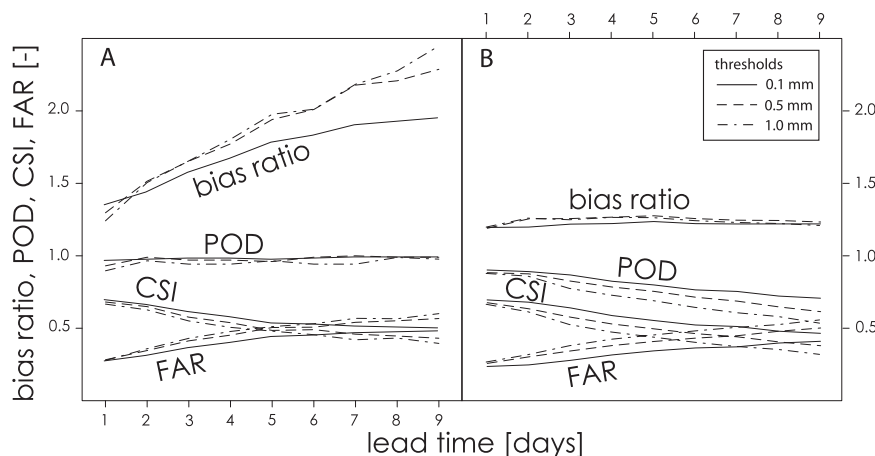

FIG. 7. Categorical measures of skill for detecting rainfall using both (a) the ensemble mean and (b) the ensemble members of the rainfall forecast.
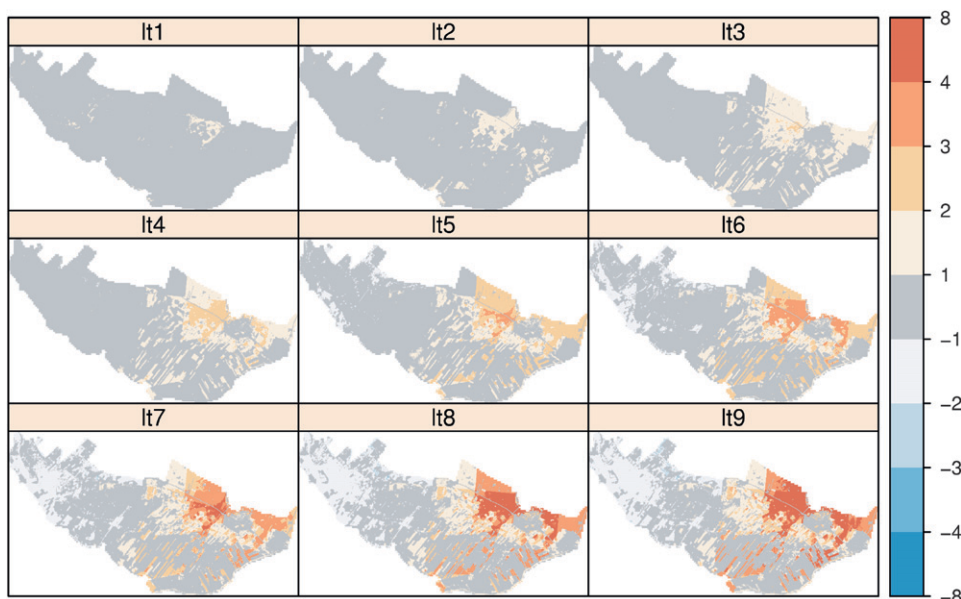
FIG. 8. Temporal mean bias in root zone storage during March–November for soil moisture forecast system I (lt1–lt9).

(location SK in Fig. 1b) the time series of storage root zone according to the true run (dotted line), according to the ensemble mean (solid line), and the range in storage root zone between the first and third quartile of the ensemble members—that is, 50% of the ensemble members, gray bound). Figure 11 shows this for four lead times (lt1, lt3, lt5, and lt9). This figure shows that the spread of the ensemble members of forecasted root

zone storage increases with lead time—that is, the reliability of forecasted storage in root zone decreases with lead time. Also, the correlation between the forecasted and true root zone storage (dotted line) decreases with lead time; both the high and low values of storage root zone from the true run are not reproduced by the forecasts at large lead times and often show a delay.
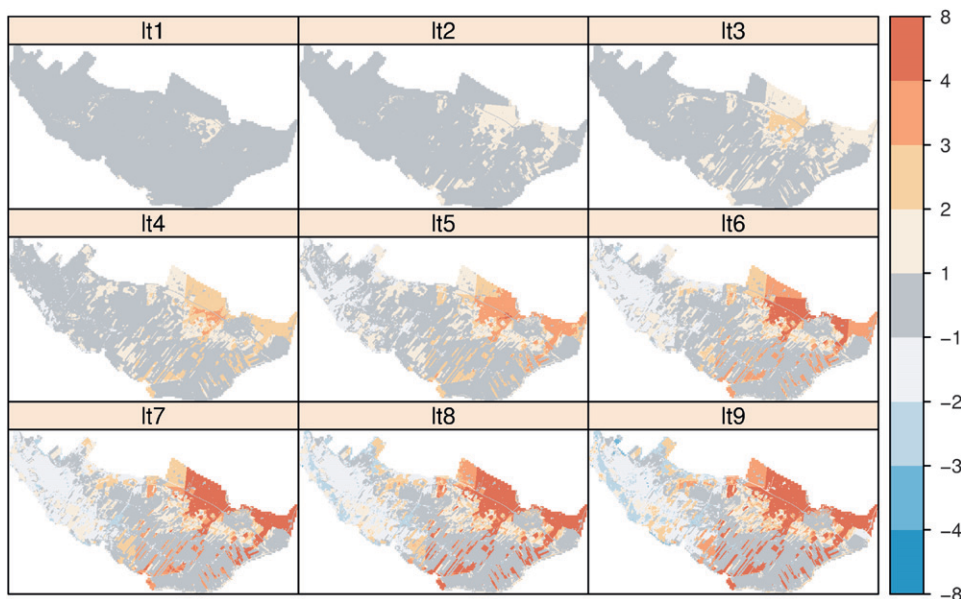

FIG. 9. Same as Fig. 8, but for soil moisture forecast system II.

TABLE 4. Spatial mean bias, RMSE, and MAE (mm) for soil moisture forecast systems I and II vs lt.

lt	Bias(I)	Bias(II)	RMSE(I)	RMSE(II)	MAE(I)	MAE(II)
1	0.27	0.25	2.35	2.38	1.73	1.74
2	0.28	0.27	3.57	3.61	2.16	2.18
3	0.34	0.35	4.40	4.49	2.61	2.64
4	0.40	0.43	5.26	5.36	3.16	3.19
5	0.45	0.52	6.17	6.32	3.75	3.79
6	0.49	0.59	7.22	7.40	4.45	4.51
7	0.54	0.66	7.93	8.14	5.00	5.07
8	0.58	0.73	8.66	8.91	5.54	5.60
9	0.64	0.81	9.40	9.68	6.15	6.20

4. Conclusions and outlook

In the following we first list the main conclusions from this study concerning forecasted rainfall and soil moisture accuracy. Thereafter, the value for operational water management and opportunities for further research are given.

a. Forecasted rainfall accuracy

- The total amount of measured spatial mean rainfall within the study area is forecasted accurately by the ensemble mean of the rainfall forecast for all lead times (maximum difference 45 mm for lt1). However, the total measured rainfall during March–November 2006 within the study area shows a large spatial variance (200 mm). This spatial variance is not taken into account for forecasted rainfall.
- The measured rainfall (spatial mean) shows a distribution with peaks at 0–1 and >10 mm day^{-1}. These peaks are underestimated by the ensemble mean of the rainfall forecasts and this underestimation increases with lead time. The ensemble members follow more or less the distribution of measured rainfall for all lead times.
- The modeled uncertainty in rainfall by ECMWF underestimates the true uncertainty for all lead times.
- The number of rainfall events (thresholds 0.1, 0.5, and 1.0 mm day^{-1}) is overestimated (approximately 30%–40%) by the rainfall forecasts, both with the individual ensemble members as well as with the ensemble mean. This overestimation is constant with lead time for the ensemble members but increases for the ensemble mean with increasing lead time, especially for higher thresholds (up to a factor of 2–2.5 for lead time of 9 days).

b. Forecasted soil moisture accuracy

- Absolute bias values in root zone storage higher than 1 mm begin to show around a lead time of 3 days. The
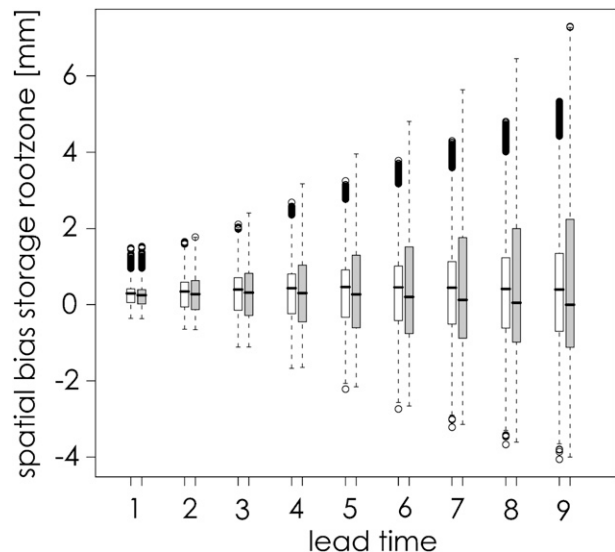

FIG. 10. Box-and-whisker plots of spatial distribution of bias in root zone storage vs lead time for soil moisture forecast system I (white) and system II (gray). The solid boxes range from the lower to the upper quartile, the black line within the box denotes the median, and dashed whiskers show the data range. Data farther than 1.5 times the interquartile range from the nearest quartile are shown as open bullets.

lower and upper bounds of bias at lead time 9 days are approximately −4 and 7 mm, respectively.
- The temporal mean bias in root zone storage shows a spatial pattern that strongly resembles the spatial pattern of total measured rainfall. This can be explained by the true run being forced with spatially variable rainfall, whereas the rainfall forecasts are spatially uniform. As a consequence, areas with less rainfall than spatial average show a negative bias and vice versa.
- Local differences occur that are superimposed on the spatial pattern of bias in root zone storage, which can be attributed to differences in land use and soil type.
- With increasing lead time, mainly the high and low values in root zone storage are not forecasted accurately and often show a delay.

c. Outlook

This study shows that the accuracy of daily ECMWF rainfall forecasts is promising and suggests that the use of these forecasts could be of value for operational water management. The main drawback of using the ECMWF ensemble rainfall forecasts to forecast the spatial distribution of soil moisture is that the rainfall forecasts are spatially uniform for most meso-γ scale—that is, 2−20 km (Orlanski 1975)—catchments. Insight into the spatial pattern of rainfall is of great importance. Additional
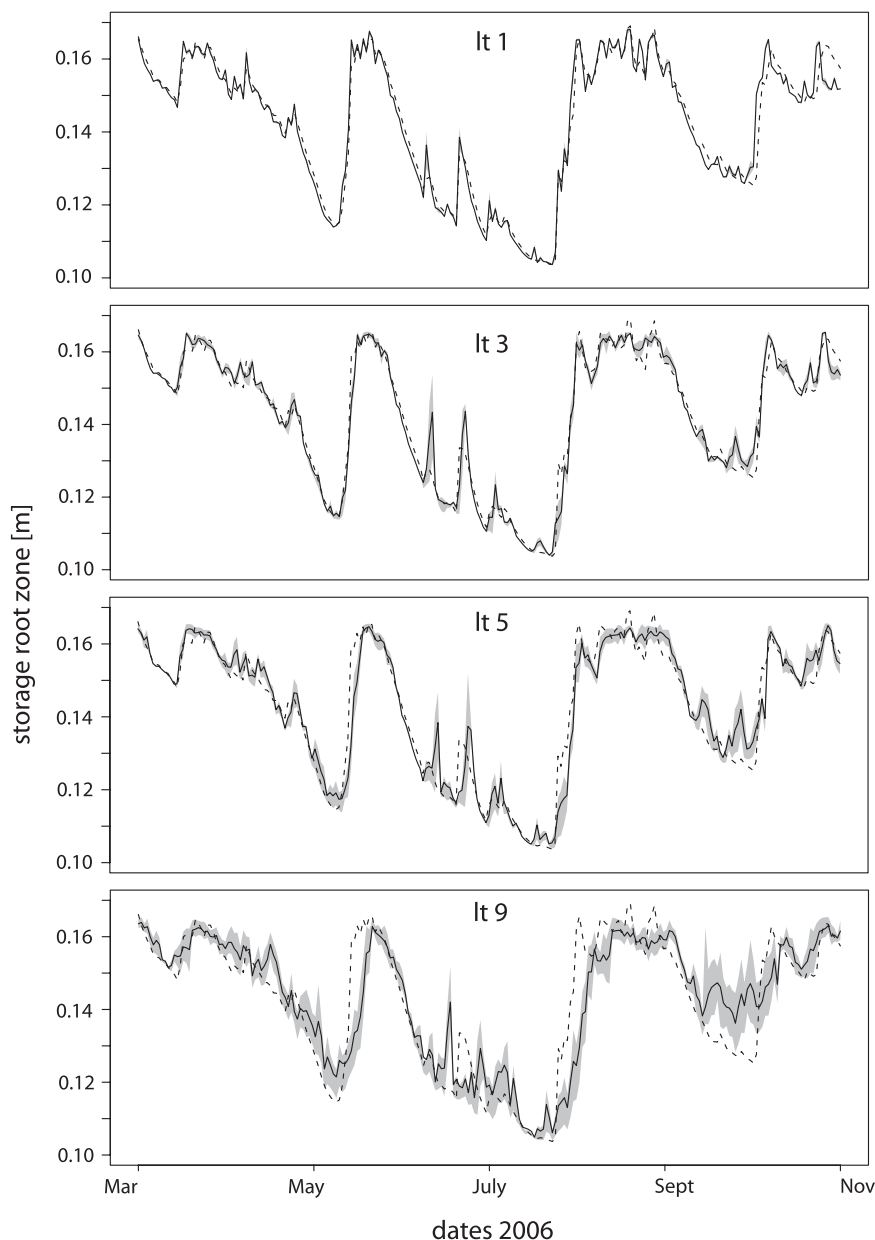
FIG. 11. Time series of root zone storage for one SVAT unit during March–November for four different lead times: (top to bottom) lt1, lt3, lt5, and lt9.

information about the spatial structure of rainfall within an area (e.g., because of orographic effects), would make it possible to downscale the rainfall forecasts, possibly leading to a decrease in the bias of forecasted root zone storage. Besides the spatial pattern in rainfall, this study shows that it is important to have good insight into the actual land use and the soil physical parameters. Finally, the input for reference evapotranspiration was set at observed values. In reality, this should be set at the forecasted values.

This study uses daily rainfall. In the Netherlands rainfall is predominantly stratiform, whereas the hydrological systems are groundwater dominated with reaction times of several days. This makes a temporal resolution of 24 h sufficient. However, for example, mountainous areas, the spatiotemporal structures of rainfall are important and the use of six hourly rainfall forecasts should be considered and investigated. Besides, for operational rainfall forecast, NWPs are not the only source. Extrapolation of radar (or satellite) precipitation patterns, for

example, also called nowcasting methods, is another source. Nowcasting methods capture the initial information almost perfectly, but because they do not include physics, the skill will decrease rapidly with lead time. NWPs, on the other hand, capture the physics of large systems very well but lack local detail because of their limited spatial resolution and have imperfect assimilation algorithms. Therefore, their skill is not so high for small lead times but decreases only gradually with increasing lead time (Golding 1998). Lin et al. (2005) investigated the crossover point in time where NWPs start to have more skill than nowcast methods and found this to be 6 h after the forecast is initiated. Although this conclusion is based on 3DVAR methods instead of 4DVAR systems (such as that of the ECMWF), qualitatively it is safe to say that if rainfall forecasts are used in hydrological studies with time steps of, for example, 1 h, a combination of nowcasting methods and NWPs should be beneficial.

REFERENCES

Berendsen, H. J. A., and E. Stouthamer, 2000: Late weichselian and Holocene palaeogeography of the Rhine-Meuse delta, The Netherlands. *Palaeogeogr., Palaeoclimatol., Palaeoecol.,* **161,** 311–335.

Bruin, H. A. R. D., 1987: From Penman to Makkink. *Evaporation and Weather: Technical Meeting 44,* J. C. Hooghart, Ed., Vol. 39, *Proceedings and Information,* TNO Committee on Hydrological Research, 5–31.

Busschers, F. S., and Coauthors, 2007: Late Pleistocene evolution of the Rhine-Meuse system in the southern North Sea basin: Imprints of climate change, sea-level oscillation and glacio-isostacy. *Quat. Sci. Rev.,* **26,** 3216–3248.

de Wit, A. J. W., and J. G. P. W. Clevers, 2004: Efficiency and accuracy of per-field classification for operational crop mapping. *Int. J. Remote Sens.,* **25,** 4091–4112.

Golding, B. W., 1998: Nimrod: A system for generating automated very short range forecasts. *Meteor. Appl.,* **5,** 1–16.

Gouweleeuw, B. T., J. Thielen, G. Franchello, and A. P. J. D. Roo, 2005: Flood forecasting using medium-range probabilistic weather prediction. *Hydrol. Earth Syst. Sci.,* **9,** 365–380.

Johnson, L. E., and B. G. Olson, 1998: Assessment of quantitative precipitation forecasts. *Wea. Forecasting,* **13,** 75–83.

Lin, C., S. Vasić, A. Kilambi, B. Turner, and I. Zawadzki, 2005: Precipitation forecast skill of numerical weather prediction models and radar nowcasts. *Geophys. Res. Lett.,* **32,** L14801, doi:10.1029/2005GL023451.

Makkink, G. F., 1957: Testing the panman formula by means of lysimeters. *J. Inst. Water Eng.,* **11,** 277–288.

McDonald, M. G., and A. W. Harbaugh, 1984: A modular three-dimensional finite-difference ground-water flow model. U.S. Geological Survey Open-File Rep. 83-875, 539 pp.

Olsson, J., and G. Lindström, 2008: Evaluation and calibration of operational hydrological ensemble forecasts in Sweden. *J. Hydrol.,* **350,** 14–24.

Orlanski, I., 1975: A rational subdivision of scales for atmospheric process. *Bull. Amer. Meteor. Soc.,* **56,** 527–530.

Pappenberger, F., K. J. Beven, N. M. Hunter, P. D. Bates, B. T. Gouweleeuw, J. Thielen, and A. P. J. D. Roo, 2005: Cascading model uncertainty from medium range weather forecasts (10 days) through a rainfall-runoff model to flood inundation predictions with the European Flood Forecasting System (EFFS). *Hydrol. Earth Syst. Sci.,* **9,** 381–393.

Persson, A., 2001: User Guide to ECMWF forecast products. ECMWF Meteorology Bulletin M3.2., 123 pp.

Roo, A. D., and Coauthors, 2003: Development of a European flood forecasting system. *Int. J. River Basin Manage.,* **1,** 49–59.

Roulin, E., 2007: Skill and relative economic value of medium-range hydrological ensemble predictions. *Hydrol. Earth Syst. Sci.,* **11,** 725–737.

——, and S. Vannitsem, 2005: Skill of medium-range hydrological ensemble predictions. *J. Hydrometeor.,* **6,** 729–744.

Schuurmans, J. M., and M. F. P. Bierkens, 2007: Effect of spatial distribution of daily rainfall on interior catchment response of a distributed hydrological model. *Hydrol. Earth Syst. Sci.,* **11,** 677–693.

——, ——, E. J. Pebesma, and R. Uijlenhoet, 2007: Automatic prediction of high-resolution daily rainfall fields for multiple extents: The potential of operational radar. *J. Hydrometeor.,* **8,** 1204–1224.

van Dam, J. C., 2000: Field-scale water flow and solute transport: SWAP model concepts, parameter estimation and case studies. Ph.D. thesis, Wageningen University, 167 pp.

van Oort, P. A. J., A. K. Bregt, S. de Bruin, A. J. W. de Wit, and A. Stein, 2004: Spatial variability in classification accuracy of agricultural crops in the Dutch national land-cover database. *Int. J. Geogr. Inf. Sci.,* **18,** 611–626.

van Walsum, P. E. V., and P. Groenendijk, 2008: Quasi steady-state simulation of the unsaturated zone in groundwater modeling of lowland regions. *Vadose Zone J.,* **7,** 769–781.

Winter, T. C., D. O. Rosenberry, and A. M. Sturrock, 1995: Evaluation of 11 equations for determining evaporation for a small lake in the north central United States. *Water Resour. Res.,* **31,** 983–993.

Wösten, J. H. M., F. de Vries, J. Denneboom, and A. F. van Holst, 1995: Generalization and soil physical translation of the Dutch soil map, 1:250.000, on behalf of the PAWN study (in Dutch). Foundation for Soil Mapping Rep. 2055, 50 pp.